Supplementary Information

The collagen-binding protein of *Streptococcus mutans* is involved in hemorrhagic stroke

Kazuhiko Nakano, Kazuya Hokamura, Naho Taniguchi, Koichiro Wada†, Chiho Kudo, Ryota Nomura, Ayuchi Kojima, Shuhei Naka, Yoshinori Muranaka, Min Thura, Atsushi Nakajima, Katsuhiko Masuda, Ichiro Nakagawa, Pietro Speziale, Nobumitsu Shimada, Atsuo Amano, Yoshinori Kamisaki, Tokutaro Tanaka, Kazuo Umemura, and Takashi Ooshima.

†Address correspondence to Dr. Koichiro Wada,
Department of Pharmacology, Osaka University Graduate School of Dentistry,
1-8 Yamada-oka, Suita, Osaka 565-0871, Japan.
Tel: +81-6-6879-2913; Fax: +81-6-6879-2914;
E-mail: kwada@dent.osaka-u.ac.jp.

Supplementary information includes:

Supplementary Figures S1 to S8,

Supplementary Tables S1 to S4,

Supplementary Figures

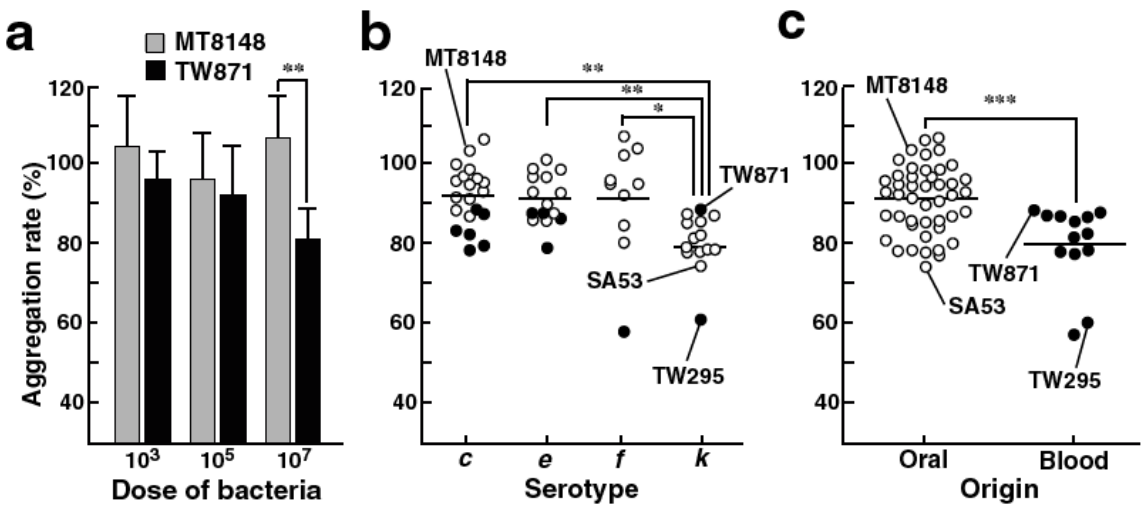

Supplementary Figure S1: Effect of various *S. mutans* strains on platelet aggregation. (**a**) The aggregation rates of MT8148, a standard strain, or TW871, a virulent strain, with various bacterial cell numbers. Whole blood aggregation was measured by an impedance method with a whole-blood aggregometer (C540, Baxter Ltd., Tokyo, Japan). Various concentrations of bacterial cells (final concentration was 10^3, 10^5, or 10^7cells/mL) were added to whole blood collected from mice. The whole blood was incubated at 37℃ for 5 min, followed by the addition of collagen (4 μg of native collagen fibrils, type I). Aggregation rates of each strain were calculated by maximum impedance (Ω) values during the 20 min. observation period with or without the addition of bacterial cells, and were expressed as percent of aggregation in comparison to vehicle control. Each column represents mean ± standard deviation (SD) from 3-5 independent experiments. Statistical significance was determined using Student's t-test. $^{**}p < 0.01$ versus MT8148. (**b**) Platelet aggregation rates on various serotypes of *S. mutans*. Platelet aggregation rates in 58 clinical strains were evaluated by the same method described in (a). The results were shown based on serotypes (*c*; n=20, *e*; n=15, *f*; n=10, and *k*; n=13) or origin of the isolates. Statistical significance was determined using Fisher's PLSD test. $^{*}p < 0.05$, $^{**}p < 0.01$. (**c**) Comparison of platelet aggregation rates between oral and blood isolates (oral; n=45, and blood; n=13). Open and closed circles indicate the oral and blood isolates, respectively. Horizontal thick bars indicate the mean values of each group. Statistical significance was determined using Student's t-test ($^{***}p < 0.001$).

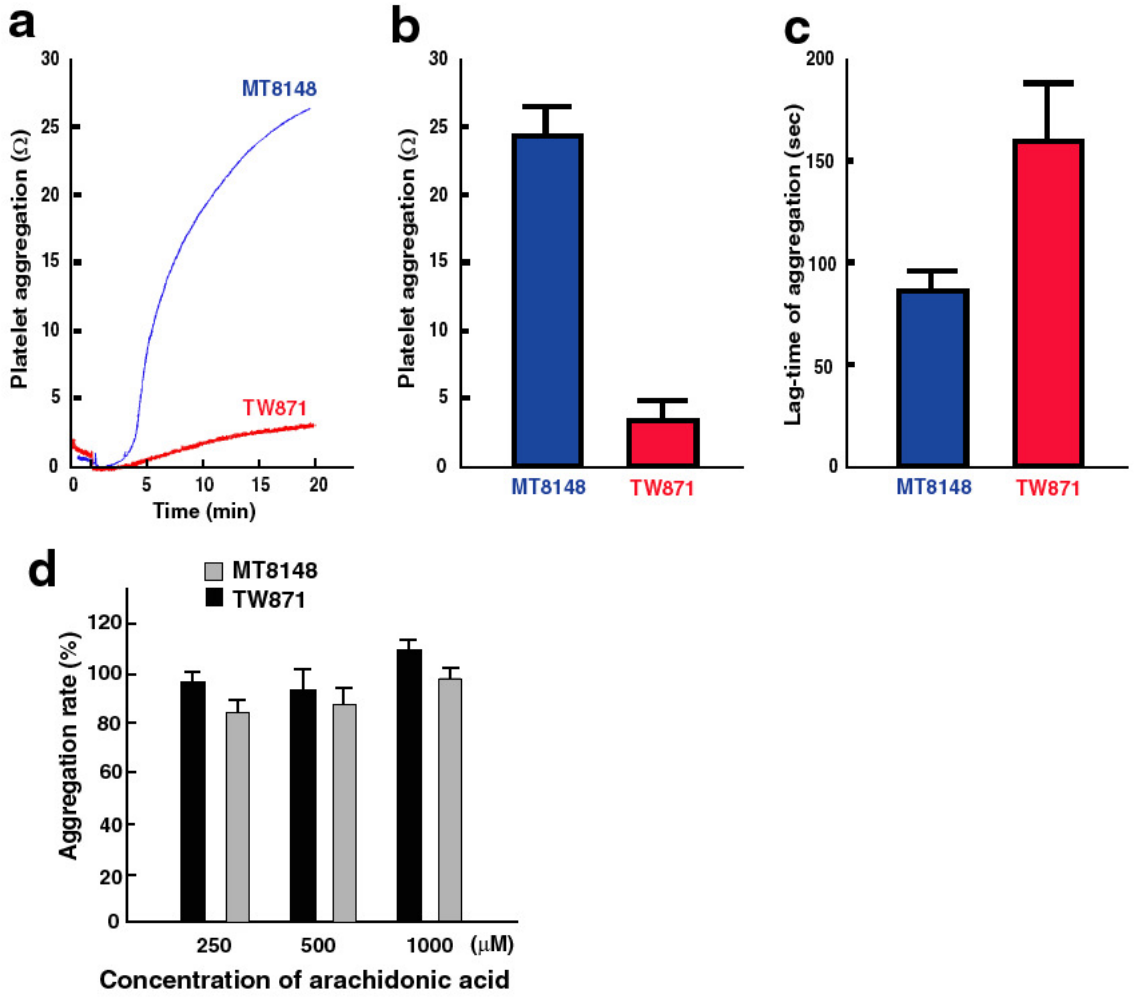

Supplementary Figure S2: Effect of serotype *k S. mutans*, TW871, on platelet aggregation. (**a**) Representative chart of platelet aggregation assay using human platelet-rich plasma (PRP). Human PRP was prepared from healthy volunteers. Platelet aggregation was evaluated in human PRP incubated with the standard *S. mutans* strain, MT8148, or TW871 (final concentration was 10^7cells/ml). Collagen (4 μg) was added at 5 min and the maximum impedance value during a 20 min observation period was measured. (**b**) Maximum platelet aggregation rates with MT8148 or TW295 were evaluated using PRP by the same method described in (a). Each column represents mean ± SD from 3–4 independent experiments. (**c**): Prolongation of lag-time of platelet aggregation by TW871. The lag-time of platelet aggregation after the addition of collagen was measured by the same method described in (a). Each column represents mean ± SD from 3–4 independent experiments. (**d**) Effect of bacteria on arachidonic acid-induced platelet aggregations. Arachidonic acid was used as the aggregation reagent instead of collagen on whole blood aggregation. Each column represents mean ± SEM from 8–14 independent experiments.

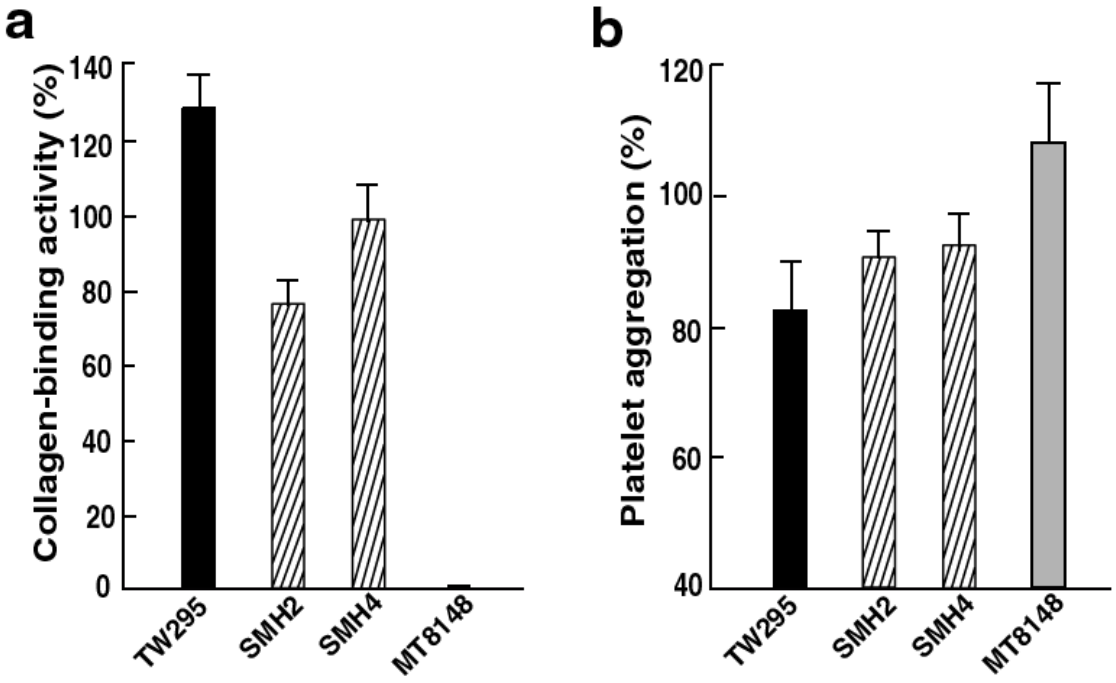

Supplementary Figure S3: Effect of bacteria isolated from human stroke patients on collagen-binding activity and platelet aggregation. (**a**) Collagen-binding activity of *S. mutans* strains (SMH2 and SMH4) isolated from stroke patients. The activity was evaluated under fixed conditions of 2 mg of Type I collagen and $1x10^{10}$ bacterial cells. The results for each strain are expressed as a percentage based on that of TW871, defined as 100%. Each column represents mean ± SD from 3–4 independent experiments. (**b**) Platelet aggregation activity of *S. mutans* strains isolated from stroke patients. The assays were performed using whole blood obtained from mice by an impedance method with an aggregometer under the fixed condition of 4 µg of Type I collagen and $1x10^{7}$ bacterial cells. The results for each strain are expressed as a percentage based on the samples with collagen but no bacterial cells, defined as 100%. Each column represents mean ± SD from 3–4 independent experiments.

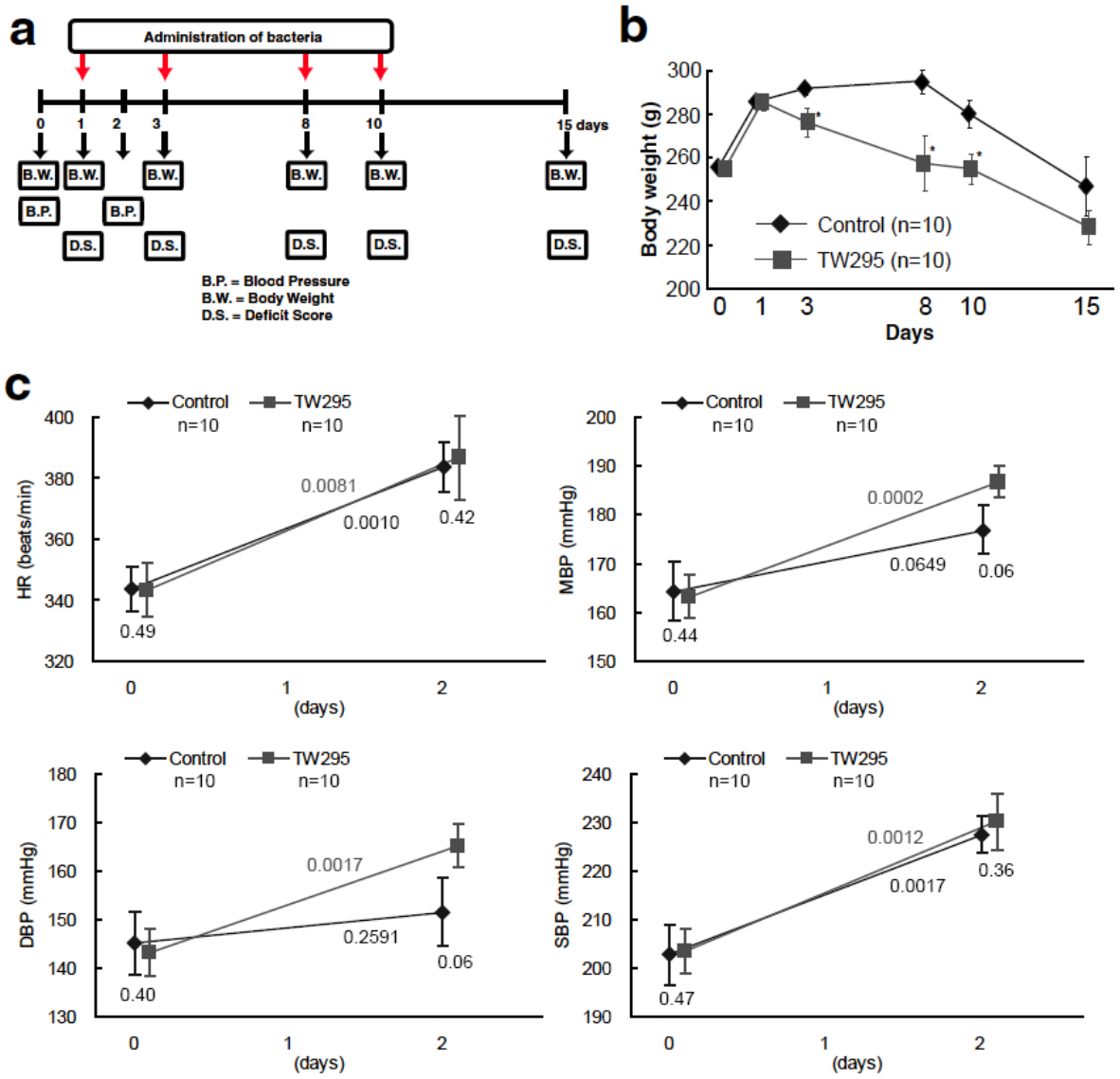

Supplementary Figure S4: Effect of TW295 on stroke prone spontaneous hypertensive (SHRSP) rats. (**a**) Schedule of experimental procedures. Administration of bacteria was performed at day 1, 3, 8, and 10. Various parameters such as body weight (B.W.), blood pressure (B.P.), and deficit score (D.S.), an index of neurological dysfunction, were evaluated until day 15. (**b**) Alterations of body weight in control and TW295-administered SHRSP rats. A significant decrease in the body weight of TW295-administered SHRSP rats was observed in comparison to that of vehicle-administered control SHRSP rats. Each point represents mean ± SEM from 10 independent animals. (**c**) Comparison of blood parameters between control and TW295-administered rats. Heart rate (HR), mean blood pressure (MPB), diastolic (DPB) and systolic blood pressure (SBP) were measured. Each point represents mean ± SEM from 10 independent animals.

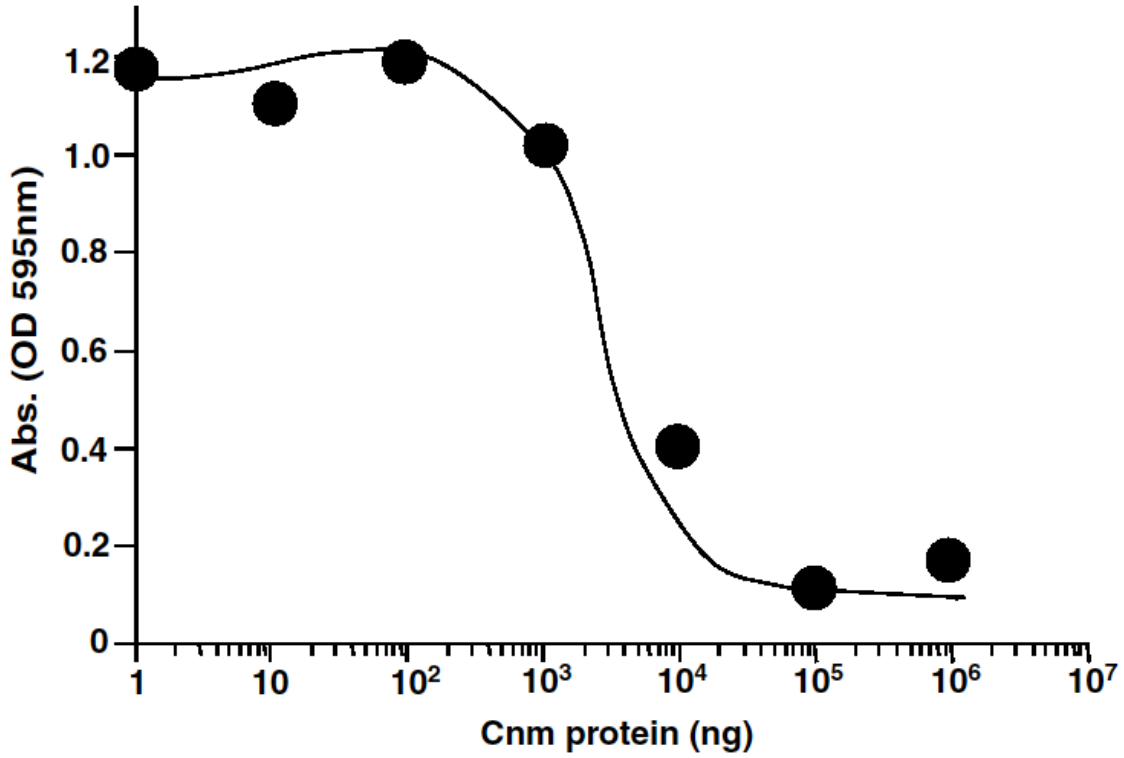

Supplementary Figure S5: Dose-dependent effect of recombinant Cnm protein on TW295 adhesion to a collagen layer *in vitro*. Each dosage of recombinant Cnm protein was coated onto collagen layer plates and TW295 bacteria ($1x10^7$ cells) were applied to the collagen layer plates. The amount of adherent TW295 bacteria was determined by measurement of OD 595 nm absorbance. Pretreatment of recombinant Cnm protein completely inhibited adhesion of TW295 to the collagen layer, indicating the adherent ability of 100000 ng (100 μg) of recombinant Cnm protein is almost equal to that of $1x10^7$ TW295 cells. Each point represents the mean value from 3 independent experiments.

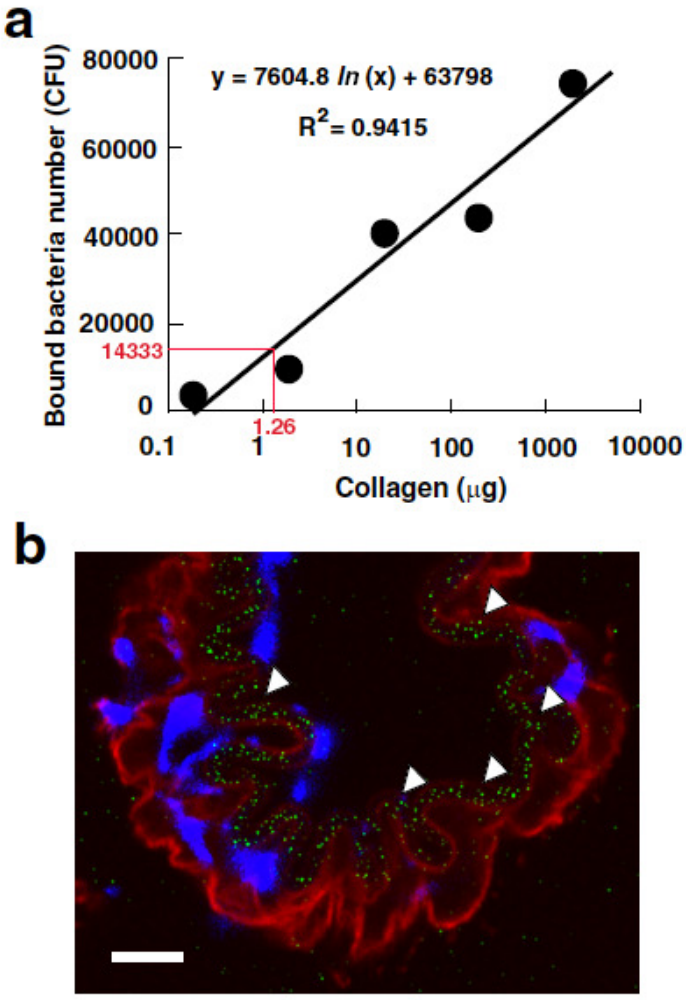

Supplementary Figure S6: Relationship between exposed collagen and bacteria bound to the collagen layer. (**a**) Relationship between the amount of collagen and the number of bacteria bound to the collagen layer in vitro. The total number of TW295 bound to the collagen-coated plate was calculated and plotted. (Regression analysis, R^2=0.9415). Red colors represent the accumulated TW295 cell number (14,333 CFU) in the ipsilateral hemisphere from the *in vivo* mouse stroke model, and the extrapolated amount of collagen (1.26 μg) exposed after endothelial cell injury in our model. (**b**) Interaction of TW295 with a damaged blood vessel. A green fluorescent protein (GFP)-expressing TW295 strain was administered to a hemorrhagic mouse model and the ipsilateral hemisphere was collected. The damaged area of the ipsilateral hemisphere was immunohistochemically stained with anti-collagen type IV antibody, and counterstained with DAPI. Green, red, and blue color represents TW295 cells, collagen layer, and nuclei of endothelial cells, respectively. White arrowheads represent the TW295 bacteria that bound to the exposed collagen layers where endothelial cells were ruptured. Scale bar; 5μm.

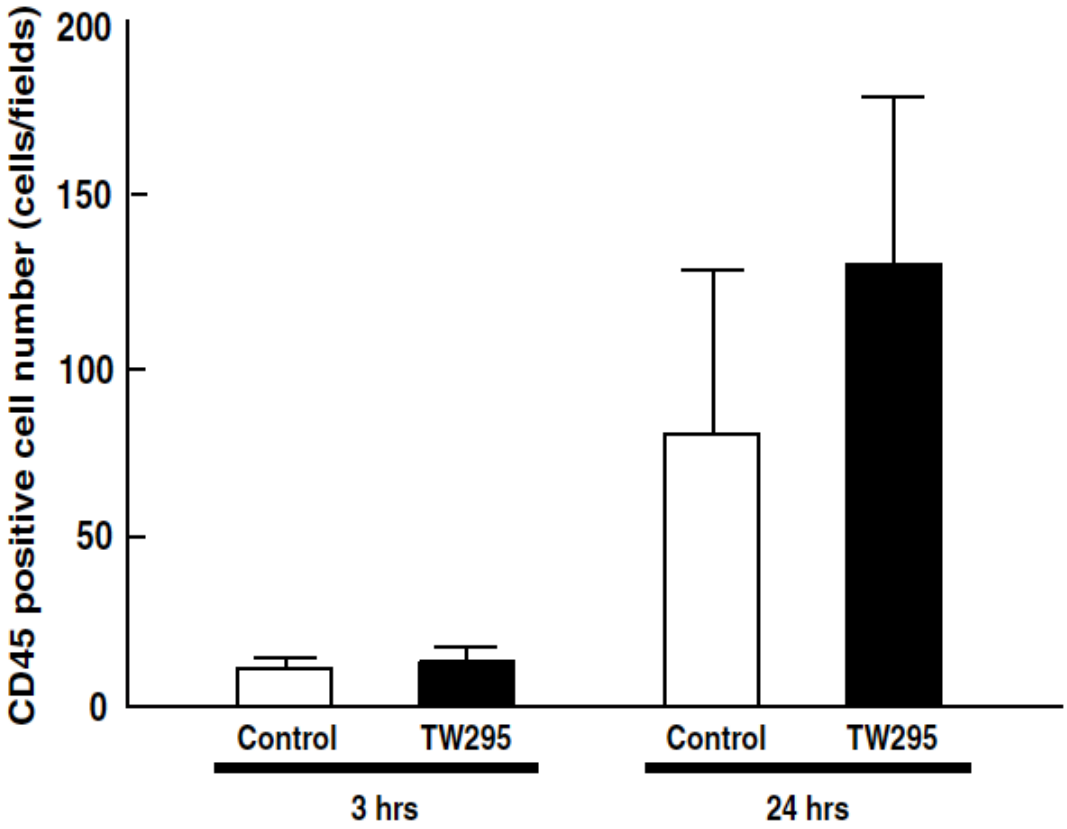

Supplementary Figure S7: Effect of TW295 on leukocyte infiltration in a cerebral hemorrhage model. Three or 24 hours after the onset of cerebral hemorrhage, ipsilateral mouse brain was formalin fixed and embedded in paraffin. Sections were stained with the CD45 antibody (pan-leukocyte marker), and CD45-positive cell number was counted in three fields (20x10 magnification) on each sample. A tendency for increased CD45-positive cell number was observed in TW295 administered mouse brains at 24 hrs in comparison to vehicle control. Each column represents mean ± SD from 3 independent experiments.

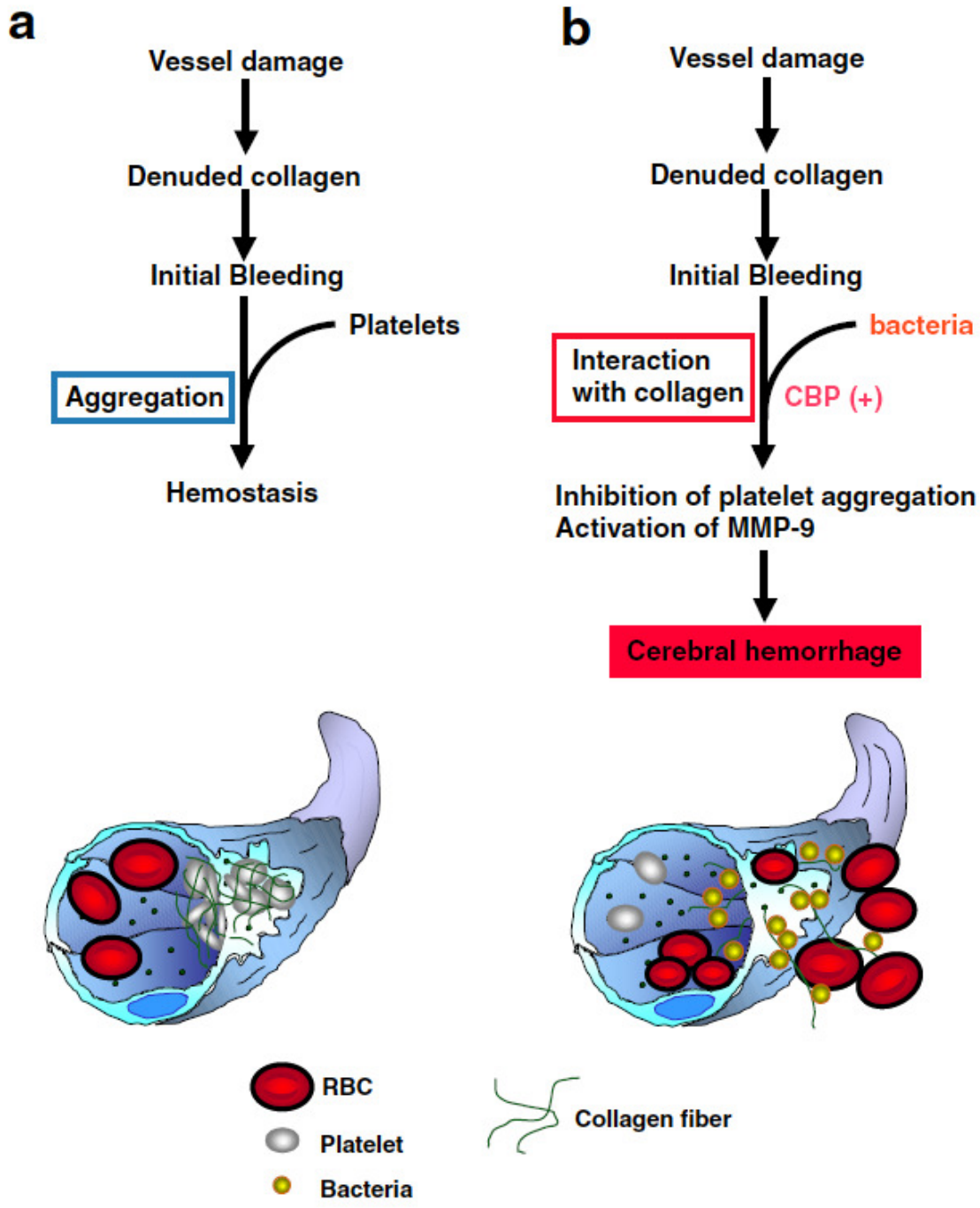

Supplementary Figure S8: Schematic illustration of the putative mechanism for the aggravation of cerebral hemorrhage by *S. mutans* cells. (**a**) Normal hemostasis caused by platelet aggregation on the location of endothelial damage. (**b**) *S. mutans* cells with the properties of highly negative charge accumulate on exposed collagen with positive charge, and those with collagen-binding proteins have a high affinity to exposed collagen, both of which lead to activation of MMP-9 and inhibition of collagen-induced platelet aggregation at the site of endothelial damage, causing persistent bleeding.

Supplementary Tables

Supplementary Table S1: *S. mutans* strains used in this study.

Strains	Serotypes	Cnm expression	Features	References
TW295	*k*	Cnm (+)	Blood isolate from Japanese subject with bacteremia after tooth extraction	(14), (16)
TW295CND	*k*	Cnm (-)	Isogenic mutant with Cnm defect constructed from TW295	(21)
TW871	*k*	Cnm (+)	Blood isolate from Japanese subject with Infective endocarditis complicated with subarachnoid hemorrhage	(14), (16)
MT8148	*c*	Cnm (-)	Oral isolate from Japanese subject	(29)
SA53	*k*	Cnm (+)	Oral isolate from Finnish subject	(20)
LJ32	*f*	Cnm (+)	Oral isolate from Japanese subject	(20)

Supplementary Table S2: Parameters of circulation in mouse hemorrhagic model.

Parameters	Time after administration (min)						
	Pre	5	10	15	20	30	40
Systolic blood pressure (mmHg)							
Control	83.0±2.5	77.3±3.7	78.0±2.0	79.7±2.8	80.3±2.6	79.0±1.5	78.0±2.5
TW295	75.5±1.3	74.3±4.8	76.0±1.0	74.3±1.4	73.3±1.4	74.5±0.9	73.8±0.6
Diastolic blood pressure (mmHg)							
Control	73.3±2.4	68.7±3.5	68.7±1.9	70.7±2.8	70.0±2.3	68.7±1.9	66.7±2.2
TW295	66.0±1.4	66.3±4.1	66.8±1.1	65.3±1.5	64.8±1.3	65.5±0.3	64.5±0.3
Mean blood pressure (mmHg)							
Control	76.0±2.1	71.7±3.4	72.7±2.4	72.7±2.3	73.3±1.8	72.3±1.5	71.0±2.1
TW295	69.0±1.0	68.8±4.7	70.0±0.4	68.5±1.2	67.3±1.3	68.8±0.9	67.3±1.1
Heart rate (beats/min)							
Control	428.3±30.6	403.0±33.8	409.3±32.7	409.3±29.8	407.7±29.8	403.0±28.0	399.3±28.1
TW295	439.0±14.5	426.0± 9.3	425.5±10.9	424.8±11.6	421.3±11.3	414.5±12.4	411.5±14.5

Data represents mean ± SEM from 3-4 independent animals. Statistical significance was determined using Student's t-test. No significant differences were observed.

Supplementary Table S3: Cerebral blood flow.

Parameters	Control	TW295
Occlusion time (sec)	396.7±126.7	469.0±101.8
Total flow time (sec)	1612.0±644.9	1749.3±287.6

Data represents mean ± SEM from 3-4 independent animals. Statistical significance was determined using Student's t-test. No significant differences were observed.

Supplementary Table S4: Comparison of frequency of *cnm*-expressing *S. mutans* infection between cerebral hemorrhage patients and ischemic stroke patients.

	Ischemic stroke patients (non-hemorrhagic)	Cerebral hemorrhage patients	P value (Fisher's exact probability test)
Total number (Male:Female)	54 (26:28)	74 (47:27)	
Age (mean±SD)	74.2 ± 9.9	68.4 ± 4.0	NS
S. mutans-isolated / total subjects (%)	27/54 (50.0%)	41/74 (55.4%)	NS
cnm-positive *S. mutans* / total hemorrhagic or non-hemorrhagic stroke patients (%)	6/54 (11.1%)	20/74 (27.0%)	$P = 0.0439$
cnm-positive *S. mutans* / total *S. mutans*- isolated subjects (%)	6/27 (22.2%)	20/41 (48.8%)	$P = 0.0410$

Oral samples were collected from multiple institutes and hospitals. Ischemic stroke patients were strictly diagnosed as ischemic stroke without any hemorrhage by MRI read by neurosurgical specialists. SD: standard deviation; NS: non-significant.

Supplementary Table S5: PCR primers used in this study.

Name	Purpose	Sequence (5' to 3')	References
MKD-F	Detection of *S. mutans*	GGC ACC ACA ACA TTG GGA AGC TCA GTT	(14), (27)
MKD-R		GGA ATG CCG ATC AGT CAA CAG GAT	
cnm-1F	Identification of *cnm*	GAC AAA GAA ATG AAA GAT GT	(20)
cnm-1R		GCA AAG ACT CTT GTC CCT GC	